Local reinforcing bar damage in r.c. members due to accelerated corrosion and loading

G. Mancini a, F. Tondolo [a,*], L. Iuliano [b], P. Minetola [b]

a Department of Structural, Geotechnical and Building Engineering, Politecnico di Torino, corso Duca degli Abruzzi 24, 10129 Torino, Italy
b Department of Management and Production Engineering, Politecnico di Torino, corso Duca degli Abruzzi 24, 10129 Torino, Italy

HIGHLIGHTS

Corrosion is the most common problems for reinforced concrete (r.c.) structures. Tests are performed on r.c. ties subjected to load and accelerated corrosion.

A 3D scanning system is used to obtain a model of the reinforcement reduction. A distribution of the readings is obtained.

A comparison with other tests present in literature is discussed.

ABSTRACT

Corrosion attack of steel in concrete has been studied by means of an experimental analysis on reinforced concrete ties under both static/cyclic loading and accelerated corrosion. Crack opening zones across crack locations due to load have been analysed; corrosion concentration around crack site has been observed. A quantitative evaluation of local damage is presented by means of a mechanical procedure using 3D scanning and data post-processing.

The results show the influence of the presence of corrosion, stress amplitude and the type of loading on local damage. A comparison with other results found in literature is shown.

Keywords:
Corrosion
Concrete
Attack penetration
Accelerated corrosion
Pitting
Structural effect

1. Introduction

Reinforced concrete (r.c.) elements can be damaged by reinforcement corrosion in different ways, which depend on the structural characteristics and environmental aggressiveness. This phenomenon is very common and the scientific community has dedicated a great deal of attention in recent years. The reason for this concern is correlated to the cost of this kind of damage, which was estimated by Koch et al. [1] to be of some points of the Gross Domestic Product for developed countries (3% in the USA) and which is likely to increase.

The corrosion of reinforcements in concrete affects r.c. structures determining a relatively uniform attack as in corrosion due to carbonation or chlorides high content; in this context, structural elements can be considered uniformly corroded along their length. In case of moderate chloride content induced corrosion, the degradation phenomenon is generally localized. However, even where uniform corrosion is expected, important localizations can be present [2,3] and these need to be examined carefully. A concentrated attack and its quantitative evaluation are key aspects, since the structural behavior of an r.c. elements is closely related to its sectional and local bond conditions. In particular, considering the material scale, the ductility of reinforcing bars can be drastically impaired because of corrosion attack and its variability. Cairns et al. [4] stated that bars subjected to local or pitting attack may suffer a relatively modest loss of strength, but a significant loss of ductility was also evidenced. Reduced material ductility has a direct effect on the structural response and, in particular, deter-mines a reduction in the overall structural deformation capacity of a structural element. This phenomenon has been highlighted in several papers [5–9] in which r.c. elements, under different lev-els of corrosion attack, were loaded from the service load level to collapse in order to characterize the structural response.

* Corresponding author. Tel.: +39 011 090 4827.
E-mail address: francesco.tondolo@polito.it (F. Tondolo).

Some papers on r.c. elements subjected to both natural corrosion due to chlorides (Zhang et al. [10], Gonzalez et al. [11], Torres-Acosta and Miguel-Madrid [12]) and accelerated corrosion (Rodriguez et al. [3], Almusallam et al. [6]) are present in the literature. The effect of corrosion produced by means of accelerated methods may differ from that of natural corrosion, in terms of produced oxides, the physics of formation, the expansion and the internal pressure release due to oxide flow within the micro-pores and the capillarity of concrete; the slowness in the natural phenomenon and the need for a methodical approach have encouraged researchers to use accelerated corrosion methods. Therefore, together with a few tests on natural corroded elements, a huge number of tests have been performed on artificial corroded specimens in order to benefit from a systematic approach to the study of the chemical, physical and mechanical aspects. Galvanostatic methodologies are employed for the accelerated corrosion method; an electrical current density flowing in the reinforcement determines the formation of different types of oxides. Some studies refer to the total amount of penetration, which depends on the time and current density, and are essentially based on Faraday's law [13]. They have considered the effectiveness of electrochemical methods by reviewing experimental tests. Some other studies [14–19] used this methodology to rapidly simulate the following items in a controlled manner: cracking of concrete due to the lat-eral pressure increase caused by oxide formation in function of the geometrical and mechanical parameters, variation in the bond between steel and concrete in the presence of corrosion and static or cyclic loading [20] and finally structural behavior for reinforced and prestressed concrete corroded members. As far as corrosion rates are concerned, in Alonso et al. [21] and El Maaddawy and Soudki [13] it is suggested not to surpass values in the 100–200 μA/cm^2 range in order to produce similar structural effects to those produced by natural corrosion. Saifullah and Clark [22] suggested a higher corrosion rate than 250 μA/cm^2 could have a negative effect on the structural behavior due to some spurious bond deterioration. Furthermore cracking due to direct and indi-rect actions can influence the evolution and morphology of corro-sion attack, since the availability of oxygen and moisture are critical for the rate of propagation. However some researches have pointed out that the presence of crack openings does not have a marked effect on the corrosion rate [23] or on the corrosion pattern if the cracks remain within 0.3–0.5 mm, when there is an adequate concrete cover. This is essentially due to the sealing effect of oxides which, like gel, flow within the crack edges filling and protecting the crack from further moisture and oxygen ingress. Tests on the effect of corrosion, in terms of localization, have been conducted in the past. Rodriguez et al. [15] gave an average value and a stan-dard deviation of corrosion penetration and proposed a rough but effective formula for its estimation. More detailed distributions have been provided in Zhang et al. [10], who analyzed and documented many reinforcing bar segments. Torres Acosta and Martinez Madrid [12] have analyzed the local effects of corrosion and have linked the extent linking the amount of corrosion penetration to a reduction in bearing capacity of the r.c. members. It is also possible to obtain another statistical description of the damage of reinforcing bars, for concrete under marine environment from this work. All the previous results were based on tests in which the mechanical actions were negligible or constant during the corrosion period and where the previous mentioned sealing effect of corrosion was feasible.

If a variable cyclic action, due to loading, is present, a corresponding modification of the crack opening can be expected and completely different conditions would be determined. Bridges or other structural members in which the sealing effect of corrosion products within a crack is periodically destroyed by deformations are usually characterized by these conditions. Furthermore this opening and closing mechanism expose the virgin steel material of reinforcements to direct contact with external agents. Considering all the reasons described above, it is evident that a need exist to analyze the effects of corrosion on reinforcing bars and in particular the local penetration of corrosion on elements subjected to different loading patterns and simultaneous corrosion.

2. Specimens and test procedure

2.1. Materials and definition of the geometry

The structural elements used in the test were r.c. specimens. The dimensions of the specimens are reported in Fig. 1a and b. The reinforcement was a grade B450C according to Italian Code [24]. A common Portland cement type was used to cast the concrete. The compressive strength of the concrete at 28 days was equal to 25.2 MPa. 3% of NaCl by weight of cement was added in order to ensure reinforce-ment depassivation and prepare the reinforcement for electrochemical corrosion. The set-up of the mechanical testing and corrosion process is reported in Fig. 1c. The specimen was fixed within the clamping jaws of an MTS machine and tested under tension.

The different load levels and mechanical test types (static or cyclic) are reported in Table 1. The specimens, other than being mechanically impaired, were also subjected to an electrochemical corrosion mechanism. A power supply was connected to the steel bar, which acted like an anode, and 4 stainless steel plates (AISI 304), connected to the specimen sides, with the interposition of stainless steel wool, acted like cathodes around the sample. A current density of 200 μA/cm^2, together with daily wet and dry cycles, were applied and, after 25 days of application, a cor-rosion pattern equal to about 27 years of corrosion attack in an XC4 environment exposure class [25] was obtained. This simulation procedure is based on the assumption that a constant electrical current density, n-times higher than that measured in the specific environmental conditions (class XC4), produces a linear effect, over time, which is n-times faster than in real conditions.

More details about the whole experimental campaign and test set-up can be found in Giordano et al. [17].

A total of 5 specimens are analyzed here and in particular their reinforcing bars; these specimens correspond to the corroded samples that were tested during the experimental campaign. The experimental survey was mainly focused on crack widths and uncorroded specimens were also tested for comparison purposes. No differences were registered for the uncorroded specimens in terms of reinforcing bar degradation as no corrosion damage was induced. The tested specimens are listed in Table 1. The first column refer to the specimen name, in which the prefix "F" means fatigue/cyclic load, the first two digits refer to the maximum load reached during the loading phase, which is also reported in the third column, and the last two digits pertain to the amplitude of the stress variation in the reinforce-ment steel in MPa, which is also reported in the fourth column in terms of kN. The cyclic load was induced by means of a sinusoidal input, with a frequency of 3 Hz; this value was chosen on the base of a structural analysis of the stress variation in a cantilever slab element of a highway bridge under fatigue load model 3 [26]. About 6.5 million cycles had been concluded at the end of the test, that is, after 25 days. Three different loading levels, corresponding to transversal reference con-crete crack openings, measured at the beginning of the test, of 0.15, 0.20, 0.25 mm, respectively, were studied. The other two specimens were tested under a constant load (40 and 60 kN) and simultaneously corroded ("S" stands for static). The spec-imen with a static load equal to 33 kN was not tested because the FC33-50 speci-men showed a very low crack width level evolution compared to the other two cyclic tests; it was estimated that a negligible effect would have been observed in an SC33-00 test, in terms of crack width. The five specimens are reproduced with the transversal crack locations due to the first tensile loading in Fig. 2. A picture of the SC60-00 specimen at the end of the test is reported in the same figure. Oxide formation and the outflow of corrosion products from cracks can be observed.

After the test, each specimen was broken up and the reinforcing bar was cleaned by means of a procedure described in ASTM G1-03 2003 [27] (see Fig. 3). The calculated mass reduction was almost in line with a prediction based on Faraday's law, with a difference that was considered acceptable [17]; detailed information about the mass loss reduction is reported in the last column in Table 1.

It is important to state that the higher the load level, the higher the crack width and the higher the final value reached. Furthermore, the same increase can be observed for longitudinal cracks caused by reinforcing corrosion.

2.2. Visual results of corrosion localization

After removal of the concrete, it was clear that a concentration of corrosion was present in correspondence to both the crack location and the ends of the concrete specimens. As can be seen in Fig. 4, a very important concentration of corrosion attack is visible for specimen FC33-50. As soon as the level of load increases (FC40-50, FC60-50), the visible effect of local attack seems to be reduced. A very small concentration effect was observed for specimens subjected to a static load, a (SC40-00 and SC60-00 specimens).

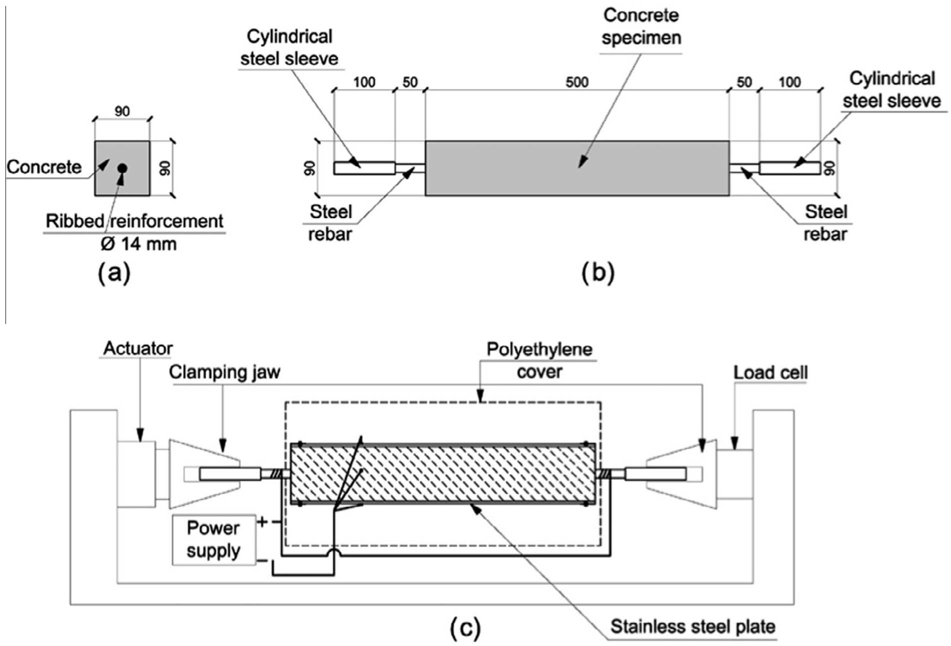

Fig. 1. (a) and (b) Specimen dimensions and (c) test set-up.

Table 1
Specimens under analysis.

Specimen	Type of load	N_{max} (kN)	ΔN (kN)	Measured mass loss (%)
FC33-50	Cyclic	33	8	4.13
FC40-50	Cyclic	40	8	5.08
FC60-50	Cyclic	60	8	5.28
SC40-00	Static	40	0	4.32
SC60-00	Static	60	0	5.05

3. Description of the analysis method

The following analysis considers some interesting points of the reinforcing bars and in particular, as can be seen in Fig. 5, the end contact points with the concrete were considered as crack locations. The steel protruding beyond the length of the concrete specimen was covered by insulating tape.

The cleaned reinforcing bars are reported in Fig. 5, for each specimen, and a trace of the concrete specimen (dashed line) is marked. The internal crack locations are evidenced with converging horizontal arrows (see Fig. 2). The names of the pieces into which each bar was cut are given on the right of each specimen, whereas the points of interest are listed on the left. Only the shaded labeled areas were analyzed by means of the 3D scanning described in the next section. Specimen FC40-50 only had one analysis point, as the zone FC40-1-2 was used for the chemical analysis on oxide products.

3.1. 3D scanning of the reinforcing bars on the points of interest

The points of interest of 18 short pieces were analyzed (Fig. 5), as it was evident, from a visual inspection, that each zone of interest was clearly limited in length across cracks within 10 mm for part. A Roland contact piezoelectric PICZA digitizer was used for the 3D scanning (Fig. 6a shows a specimen under the needle). The scan data were processed with RapidForm2006 software by Inus Technology, which is used specifically for reverse engineering activities.

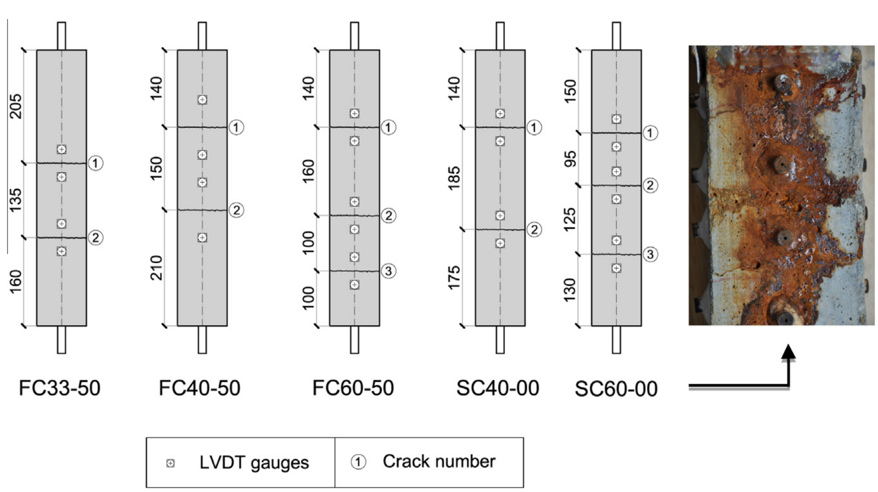

Fig. 2. Specimens with transversal loading cracks.

Fig. 3. Demolishing of the concrete specimen and cleaning of the reinforcing bar.

A detailed 3D model of the object was obtained by setting the scan point density to 20 points per millimeter. A sound piece of uncorroded and undamaged reinforcing bar of the same type as that used in the tests was first scanned and then used as a reference for the subsequent comparisons. The reference length was chosen in order to observe the profile between at least three pseudo-vertical ribs (see Fig. 6b).

The 18 corroded pieces then were scanned in 4 different positions around the central axis of the bars (see Fig. 7a), one for each 90° rotation of the piece. The real extent of the external surface of the corroded bar was obtained by means of superposition, alignment and merging of the scanned data of the 4 portions (Fig. 7b).

3.2. Comparison of the 3D data and evaluation of the corrosion extent

The evaluation of the corrosion extent was carried out for each scanned piece by conducting a refined comparison of the scanned data of the same object in two states, that is sound and corroded. Prior to the comparison, the scanned data of each corroded piece was aligned to those of the reference sound bar using a best-fitting algorithm that minimizes the deviations between couples of homologous points on the 3D models. In order to achieve better alignment of the results, the algorithm was applied after the 3D model of the reference bar was rescaled by a factor of 0.97, that is a homogeneous volumetric 3% average reduction was considered for the deformation of the bar under the tensile loading condition. The average value was computed by measuring the narrowing of the diameter of the corroded bars with respect to the corresponding diameter of the sound bar, in cross sections not affected by corrosion.

After alignment, the corroded scanned data was compared to the reference data. Signed deviations were computed using the Rapidform software and were displayed as coloured deviation maps (Fig. 8). In terms of corrosion penetration, positive values of the deviation refer to corroded areas where the surface of the corroded specimen lies below the edge of the sound reference bar. Negative values of the deviation instead indicate a swelling of the corroded specimen over the surface of the sound reference bar.

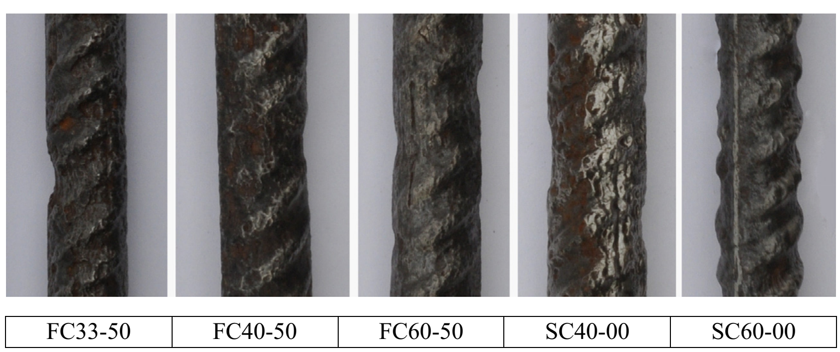

Fig. 4. Portions of the specimens under analysis.

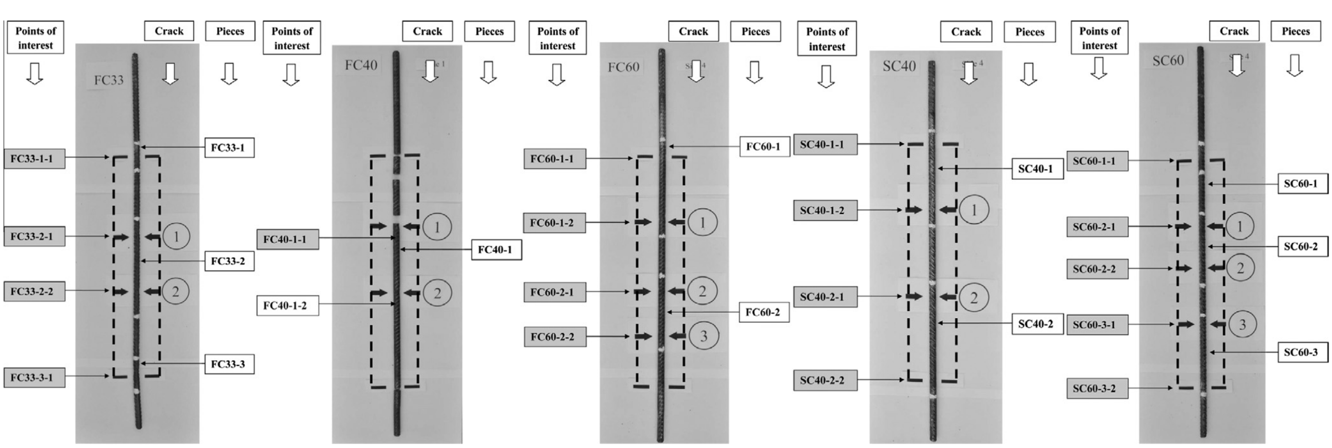

Fig. 5. Reinforcing bars after cleaning and before the 3D analysis.

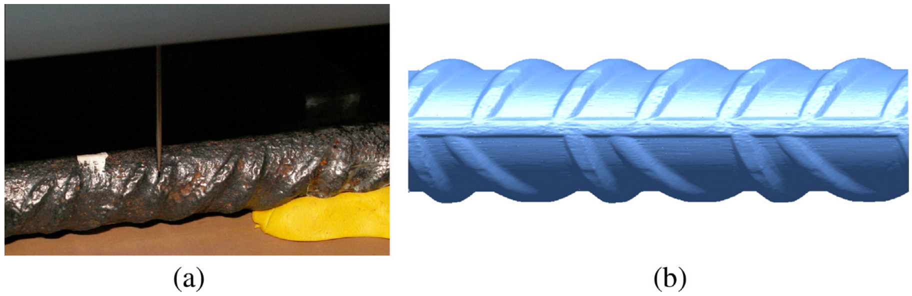

Fig. 6. Scan of a piece of bar by means of the Picza digitizer (a) and 3D model of a sound piece of bar (b).

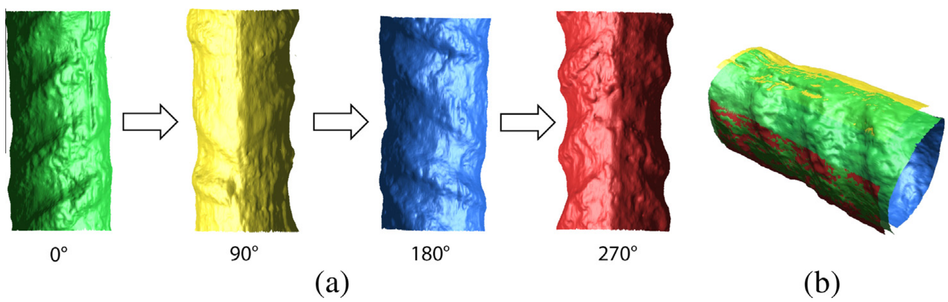

Fig. 7. 3D model of the 4 portions of the corroded bar (a) and of their superposition to obtain the exact shape of the damaged bar (b).

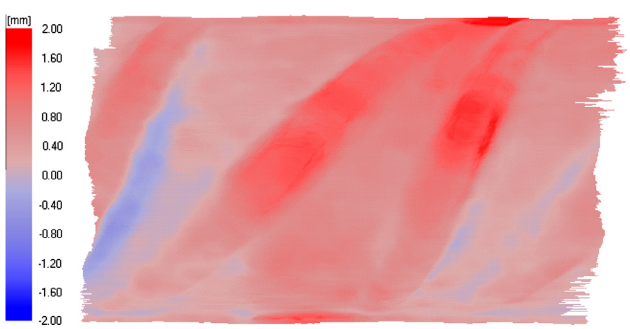

Fig. 8. Coloured deviation map of the FC60-1-2 piece.

Swelling is the consequence of the plastic deformation imposed on the bar by the tensile loading condition. However its effect is less important than that of corrosion. This can be stated as the distribution of deviations is not symmetric, but skewed towards the positive side of the plot (Fig. 9a). Moreover, the height of the negative deviation bins in the histogram is lower than that of the corresponding positive deviations for the same range of values.

The plastic deformation of a bar subjected to only a tensile stress results in such an axial displacement of the ribs that, in comparison to the sound bar, the distribution of the signed deviations is symmetric to the null value.

Therefore, the effect of corrosion was distinguished and isolated from that of the plastic deformation by first mirroring the negative part of the histogram and then subtracting the height of the mirrored bins from that of the corresponding positive deviation bins (Fig. 9b). The statistics of the modified histogram were then computed, in terms of average value (red[1] dotted line in Fig. 9), and of the standard deviation that can be associated to only the corrosion effect.

The results of this refining operation for the 18 corroded pieces are summarized in Table 2 where the statistics of the refined histogram are compared to those of the original histogram, which included the effect of the plastic deformation. Because of the skewness of the distribution, the maximum penetration depth value is slightly affected by the refining operation. This means that the value shown in the right column of Table 2 is the same for both the original and the revised distributions.

The average results calculated for the points of interest for each specimen are shown in the same table.

4. Results and discussion

The 3D analysis provides very accurate statistics of corrosion penetration in zones around the points of interest and allows a comparison to be made of specimens subjected to different types of tests and load levels which, during the experimental test, showed dissimilar crack opening patterns. Only the columns of the revised results are discussed in this section.

The outcomes, in terms of attack penetration, are reported in Table 2; it is also possible to convert these data into percentages of mass loss by means of the following equation:

$$[\%mass\ loss] = \frac{A_{ini} - A_{fin}}{A_{ini}} \cdot 100 = \frac{(2 \cdot P \cdot R - P^2)}{R^2} \cdot 100 \qquad (1)$$

where the reinforcing bar is assumed to be as a cylinder, A_{ini} is the initial transversal area of the reinforcing steel, A_{fin} is the final area after corrosion assuming a uniform reduction, P is the corrosion penetration attack and R is the initial theoretical radius of the transversal area of the reinforcing steel.

It is important to notice that the average mass loss, due to corrosion of the five specimens, which was calculated at the end of the test by weighing the steel bars, was on average 4.77% of the initial mass, and this value was very similar for each specimen (see Table 1). This value corresponds to an average attack penetration depth of 0.169 mm.

Looking at the overall general crack pattern, it can be observed that the five tested specimens showed both transversal cracks, due

[1] For interpretation of colour in Fig. 9, the reader is referred to the web version of this article.

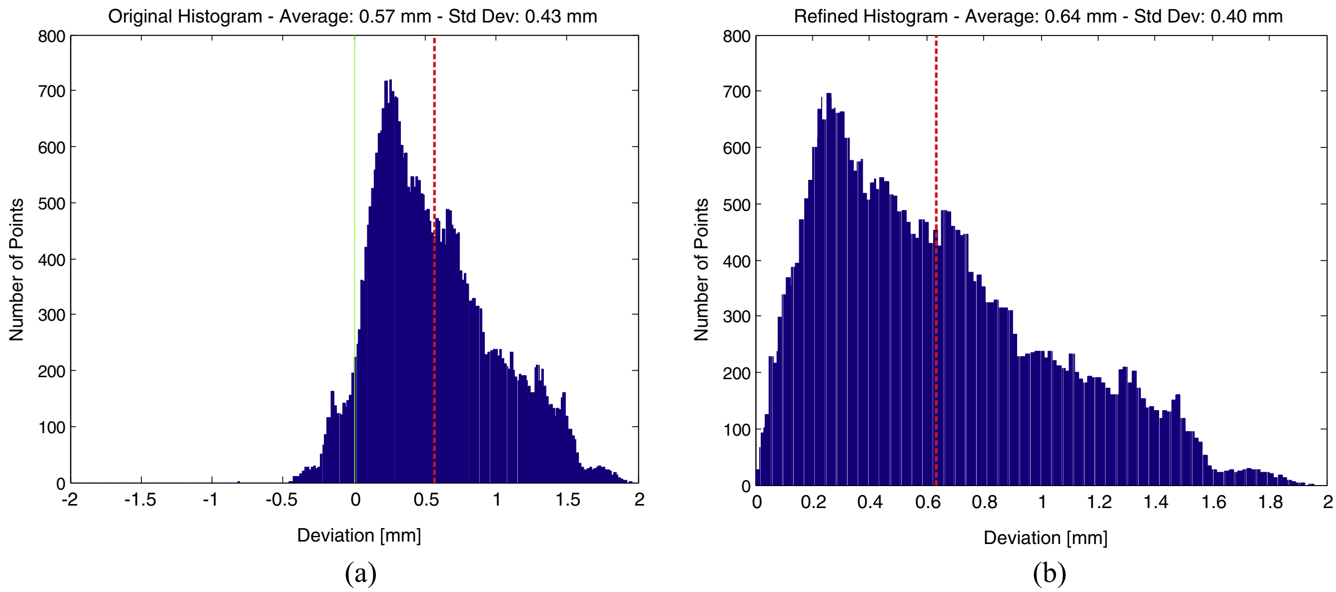

Fig. 9. Original histogram of deviations (a) and refined histogram of deviations (b) for the FC60-1-2 piece.

Table 2
Results of the 3-dimensional analysis.

	Number of points	Average penetration depth (mm)		Standard deviation (mm)		98th percentile (mm)		Maximum measured value (mm)
		Original	Revised	Original	Revised	Original	Revised	
FC33-1-1	384,406	0.49	0.82	0.61	0.47	1.68	1.76	2.45
FC33-2-1	260,362	0.43	0.90	0.63	0.37	1.63	1.64	2.55
FC33-2-2	257,378	0.52	0.64	0.51	0.49	1.73	1.76	2.25
FC33-3-1	258,837	0.66	0.97	0.64	0.48	1.85	1.88	3.30
FC40-1-1	256,060	0.47	0.62	0.46	0.41	1.57	1.63	2.80
FC60-1-1	245,467	0.29	0.55	0.40	0.25	1.03	1.07	1.65
FC60-1-2	241,859	0.56	0.64	0.43	0.40	1.52	1.53	2.00
FC60-2-1	243,587	0.30	0.51	0.34	0.25	0.97	1.03	1.90
FC60-2-2	389,851	0.35	0.59	0.46	0.33	1.28	1.34	2.00
SC40-1-1	358,311	0.27	0.53	0.37	0.29	1.14	1.23	1.80
SC40-1-2	274,288	0.20	0.61	0.42	0.30	1.13	1.38	2.00
SC40-2-1	265,214	0.15	0.31	0.25	0.20	0.76	0.92	1.45
SC40-2-2	269,458	0.16	0.35	0.27	0.18	0.69	0.77	1.30
SC60-1-1	394,482	0.23	0.35	0.27	0.22	0.85	0.94	1.40
SC60-2-1	350,354	0.23	0.39	0.31	0.27	1.02	1.06	1.90
SC60-2-2	396,416	0.20	0.42	0.50	0.35	1.31	1.40	2.35
SC60-3-1	259,784	0.17	0.31	0.22	0.17	0.67	0.72	1.00
SC60-3-2	235,239	0.16	0.43	0.32	0.25	0.92	0.98	1.70
Averages of mean penetration results								
FC33-50	–	0.53	0.83	0.60	0.45	1.72	1.76	2.64
FC40-50	–	0.47	0.62	0.46	0.41	1.57	1.63	2.80
FC60-50	–	0.38	0.57	0.41	0.31	1.20	1.24	1.89
SC40-00	–	0.20	0.45	0.33	0.24	0.93	1.08	1.64
SC60-00	–	0.21	0.37	0.33	0.25	0.96	1.03	1.67

to load, and longitudinal cracks caused by corrosion. The cracks due to load started with an opening value that was proportional to the loading action (33, 40 or 60 kN) and then increased proportionally over cycles for the “F” specimens or over time for the “S” specimens. Longitudinal cracks, due to corrosion, were observed on the external surface of each specimen around the 6th day of the test, and they evolved progressively in function of the load level and type of test (static or cyclic). It is important to note that application of the tensile load determined bond stresses between the steel and concrete, and also hoop stresses in the concrete around the bars that could have led to longitudinal splitting cracks; these stresses, which are similar to those due to corrosion, generated a progressive evolution of longitudinal cracking depending on the load level. Furthermore, the cyclic loading effect magnified the phenomenon, compared to static tests. As a result, the longitudinal cracks in the specimens subjected to cyclic loading showed increasing values for increasing load levels, whereas the increase was limited for the static specimens (SC40-00 and SC60-00). It can be stated that although the longitudinal crack was initially influenced mainly by corrosion, its evolution was due to both corrosion and load through bond mechanisms. This occurrence, like that of the transversal cracks (Fig. 2), led to a greater exposure of the steel bar due to the overall wider crack pattern.

The local damage around the points of interest have been analysed in terms of the average corrosion penetration value (Table 2-bottom). This value could be considered as the most representative penetration attack value of each location. In this respect, it can be noted that the average 3D scanning data of the points of interest of each reinforcing bar reveal a greater amount of corrosion on the specimen subjected to the minimum N_{max} value (FC33-50) which gradually decreases for the FC40-50 specimen and is even lower for the FC60-50 one. An average attack penetration of 0.83, 0.62 and 0.57 mm corresponding to 22.3, 16.9 and 15.6% of mass reduction was obtained, respectively, for these samples. As far as specimens SC40-00 and SC60-00 are concerned, the readings report average penetration values of 0.45 and 0.37 mm (lower than those obtained for the cyclic loading specimens with the same N_{max}). These values correspond to 12.4% and 10.3% of mass reduction. It can be observed that, for the specimens subjected to cyclic loads, that both alternate crack openings and continuous friction between the concrete and steel bar were favoured by a local increase in corrosion. In the static case, the products of corrosion, namely oxides, sealed the transversal cracks in an efficient manner. Therefore, at the points of interest, the oxygen and moisture concentration and, in general, the aggressive agents were available at the same level along the specimen for the "F" samples. Finally, it can be observed that the higher the level of the load (FC60-50), and as a consequence the initial transversal crack value, the more uniform the corrosion average attack value is along the specimen without any concentrations and the more similar to the average value of corrosion penetration (0.169 mm) occurrences. Therefore a local average corrosion penetration of more than four times the average value is registered for FC40-50 and FC60-50 specimens, whereas a huge concentration of corrosion was observed in the cracking zone which reached a value of five times the average mass loss. In this context, the key feature is undoubtedly due to cyclic action.

It is therefore evident that the concentration was higher for the FC33-50 specimen because of the reduced area available for corrosion. Instead, for the other specimens subjected to cyclic loading, the larger exposition area determined a more uniform corrosion effect along the entire reinforcing bar. The homogeneous corrosion was even more evident in the case of the static specimens.

The value of the 98 percentile of the distribution of the penetration attack and also the maximum value registered from the Picza device were obtained from an analysis of the statistics of the results. As previously mentioned, because of a possible shifting of the position of the ribs due to plastic deformation or missing alignment, the 98 percentile could be considered as a reference value of a "maximum pitting penetration". This percentile is assumed as a reliable value than the effective measured maximum one. Again in this case, as for the average values, it should be noted that the higher penetration value always pertains to the FC33-50 specimen, whereas the outcomes obtained for the other samples result to be scaled in the same manner as for the average corrosion values.

Considering the "maximum measured penetration" that is present on the specimens (see Table 2), a comparison can be made between these data, which are assumed as the maximum pit values and some previous works reported in literature. A comparison is made in Fig. 10 which takes into account the results of Gonzalez et al. [11] and those of Torres-Acosta and Martinez-Madrid [12]. The ratio between the maximum pit and the average corrosion depth (*R* parameter) was calculated. Two different conditions were suggested as the basis of the method to induce corrosion: natural and accelerated. A ratio *R* ranging between 4 and 8 was reported for natural corroded specimens, whereas an upper limit of 13 and a minimum of 5 were indicated in the case of electrochemical corrosion (density currents of 10 and 100 $\mu A/cm^2$). In Torres-Acosta and Martinez-Madrid, the ration *R* was taken equal to 7.16 as an interpolation result on the basis of various experimental tests [28,29] conducted in different corrosion environments (both natural and artificially corroded). However, 92% of the considered specimens were between a ratio of 12.5 and 4 (dotted mark in Fig. 10).

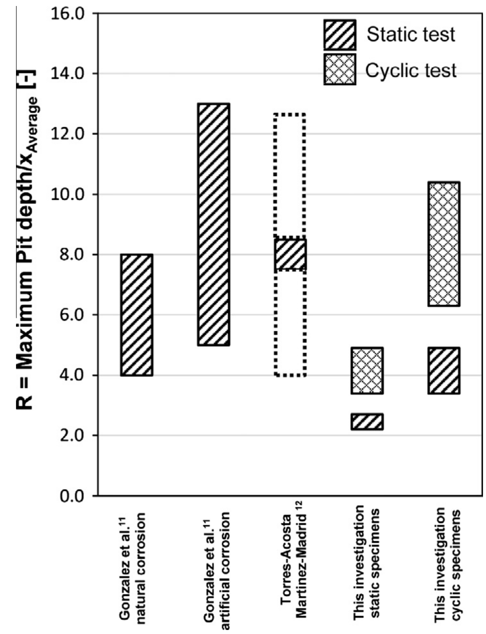

Fig. 10. *R* parameter: maximum pit depth versus $x_{average}$.

In the present investigation, the results could be divided into static and cyclic specimens, but also into average penetration values around the points of interest and maximum pits. It can be noted, for the static specimens, that penetration attack is well under the minimum values reported in the previous tests. From an examination of the pitting effect, it can be seen that only for the cyclic specimens are the values in line with the former tests, even though the latter were of a static type. According to Cairns et al. [4] the expected behavior of a corroded bar, in the presence of a uniform attack, can easily be simulated considering the residual section, whereas this behavior should be carefully evaluated in the case of a pitting attack because it can deeply impair the deformation capacity of the steel bars and, as a result, the ductility performance of both an r.c. element and a structure.

5. Conclusions

Reinforcing bars in concrete specimens have been analysed in the present work in order to locally detect their condition after they had been subjected to simultaneous loading and corrosion. Five specimens were considered from which 18 samples of reinforcing bars were investigated; three of these specimens were subjected to cyclic loading and corrosion whereas the last two were subjected to static loading and corrosion. An electrochemical method was used to induce corrosion. The present analysis was conducted after the visual inspection of the local damage observed on the steel bar specimens in correspondence to the crack location at the end of the tests.

The results point out a tendency: a very small concentration of corrosion was observed at the crack location for the samples with the static load and corrosion which resulted to be slightly more than that calculated assuming a uniform corrosion along the specimen. The concentration of corrosion is more evident in the samples subjected to both corrosion and cyclic loading. For these specimens, higher concentrations of corrosion attack were registered for lower load levels. Finally, the analysis of 98th fractile of the distributions of the penetration data evidenced a wide scatter for cyclic load tests with a low load level compared to that with the same load level but subjected to static load condition tests.

Acknowledgments

The Authors gratefully acknowledge the PhD Student Lu Liheng and the technician Piero Provenzano for having performed the experimental corrosion tests. Mention should also be made Silvia Baratelli, who performed the 3D scanning.

References

[1] Koch GH, Brongers MPH, Thompson NG, Virmani YP, Payer JH. Corrosion costs and preventive strategies in the United States. Report FHWA-RD-01-2002. p. 156.

[2] Zhang PS, Lu M, Li XY. The mechanical behavior of corroded bar. J Ind Build 1995;25(257):41–4.

[3] Rodriguez J, Ortega LM, Casal J. Load carrying capacity of concrete structures with corroded reinforcement. Constr Build Mater 1997;11(4):239–48.

[4] Cairns J, Plizzari GA, DU Y, Law DW, Franzoni C. Mechanical properties of corrosion-damaged reinforcement. ACI Mater J 2005;102(4):256–64.

[5] Castel A, Francois R, Arliguie G. Mechanical behaviour of corroded reinforced concrete beams – Part 1: Experimental study of corroded beams. Mater Struct 2000;33:539–44.

[6] Almusallam A, Al-Gahtani AS, Rauf Aziz A, Dakhil FH, Rasheeduzzafar. Effect of reinforcement corrosion o flexural behavior of concrete slabs. J Mater Civ Eng 1996;8(3):123–7.

[7] Rodriguez J, Ortega LM, Casal J, Dìez JM, Assessing structural conditions of concrete structures with corroded reinforcement. International Congress, concrete in the service of mankind, concrete repair, rehabilitation and protection, Dundee, UK, June 1996. p. 14.

[8] Mangat PS, Elgarf MS. Flexural strength of concrete beams with corroding reinforcement. ACI Struct J 1999;96(1):149–58.

[9] Shannag MJ, Al-Ateek SA. Flexural behavior of strengthened concrete beams with corroding reinforcement. Constr Build Mater 2006;20:834–40.

[10] Zhang R, Castel A, Francois R. Serviceability limit state criteria based on steel-concrete bond loss for corroded reinforced concrete in chloride environment. Mater Struct 2009;42:1407–21.

[11] Gonzalez JA, Andrade C, Alonso C, Feliu S. Comparison of rates of general corrosion and maximum pitting penetration on concrete embedded steel reinforcement. Cem Concr Res 1995;25(2):257–64.

[12] Torres Acosta A, Martinez-Madrid M. Residual life of corroding reinforced concrete structures in marine environment. J Mater Civ Eng 2003;15(4):344–53.

[13] El Maaddawy T, Soudki KA. Effectiveness of impressed current technique to simulate corrosion of steel reinforcement in concrete. J Mater Civ Eng 2003;15(1):41–7.

[14] Andrade C, Alonso C, Molina FI. Cover cracking as a function of bar corrosion: Part I-Experimental test. Mater Struct 1993;26:453–64.

[15] Rodriguez J, Ortega LM, Casal J. Corrosion of reinforcing bars and service life of reinforced concrete structures: corrosion and bond deterioration. In: International Conference "Concrete across the borders", Odense Denmark; 1994. p. 6.

[16] Ballim Y, Reid JC. Reinforcement corrosion and the deflection of RC beams – an experimental critique of current tests methods. Cem Concr Compos 2003;25:625–32.

[17] Giordano L, Mancini G, Tondolo F. Reinforced concrete members subjected to cyclic tension and corrosion. J Adv Concr Technol 2011;9(3):277–85.

[18] Giordano L, Mancini G, Tondolo F. Durability of R/C structures under mechanical and environmental action. Key Eng Mater 2011;462–463:949–54.

[19] Antonaci P, Bruno CLE, Scalerandi M, Tondolo F. Effects of corrosion on linear and nonlinear elastic properties of reinforced concrete. Cem Concr Res 2013;51:96–103.

[20] Mancini G, Tondolo F. Effect of bond degradation on existing structures – literature survey. Struct Concr, in press. doi: http://dx.doi.org/10.1002/suco.201300009.

[21] Alonso C, Andrade C, Rodriguez J, Diez JM. Factors controlling cracking of concrete affected by reinforcement corrosion. Mater Struct 1998;31(7):435–41.

[22] Saifullah M, Clark LA. Effect of corrosion rate on the bond strength of corroded reinforcement. In: Swamy RN, editor. Corrosion and corrosion protections of steel in concrete. Sheffiel: Sheffield Academic Press; 1994. p. 591–602.

[23] Mohammed TU, Otsuki N, Husada M, Shibata T. Effect of crack width and bar types on corrosion of steel in concrete. J Mater Civ Eng 2011;13(3):194–201.

[24] NTC 2008, Norme tecniche per le costruzioni. Supplemento Ordinario alla Gazzetta Ufficiale serie generale n.29 del 4 febbraio 2008, 14 January.

[25] CEN, EN 206-1 Specification, performance, production and conformity. Part 1-Concrete. Bruxelles: Comité Européen de Normalisation; 2005.

[26] CEN, EN 1991-2 Actions on structures. Part 2: Traffic load on bridges. Bruxelles: Comité Européen de Normalisation; 2005.

[27] ASTM G1-03, Standard practice for preparing, cleaning, and evaluating corrosion test specimens; 2003.

[28] Rodriguez J, Ortega LM, Casal J. Load bearing capacity of concrete columns with corroded reinforcement. In: Proc. 4th SCI Int. Symp. on corrosion of reinforcement in concrete construction, Cambridge, U.K.; 1996. p. 220–30.

[29] Tuutti K. Corrosion of steel in concrete. Stockholm, Sweden: Swedish Cement and Concrete Research Institute; 1982. p. 468.